Supplementary Figure S3: Senescent cancer cells efficiently activate dendritic cells

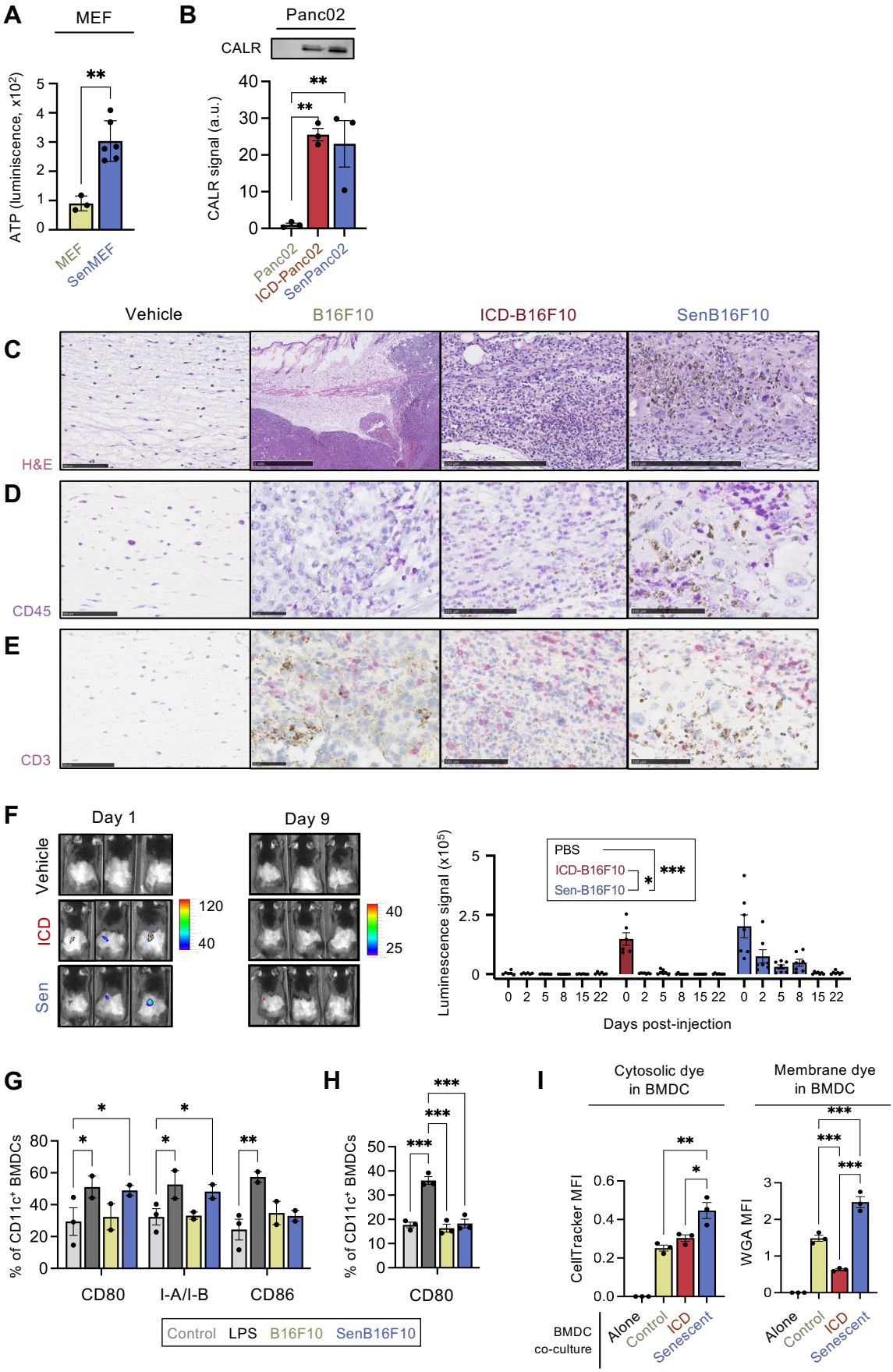

Supplementary Figure S3: Senescent cancer cells efficiently activate dendritic cells

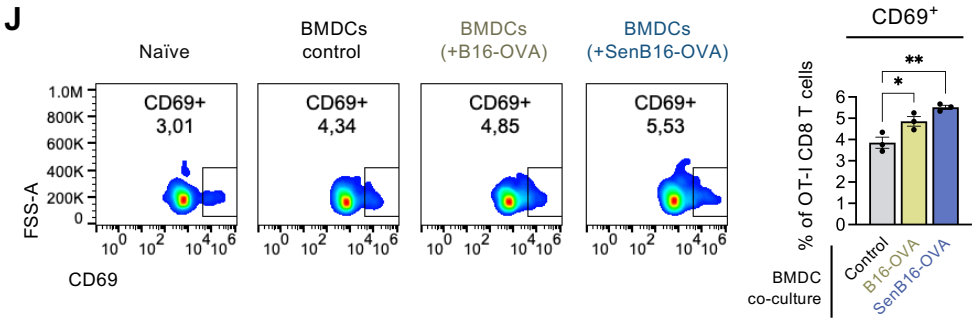

Supplementary Figure S3: Senescent cancer cells efficiently activate dendritic cells

A. Levels of extracellular ATP in the conditioned medium (CM) of 10^6 control MEF or senMEF. *n*=3 independent experiments. **p<0.01; unpaired Student's t test.

B. Immunoblot detection of CALR in the CM of 10^6 control Panc02, ICD-Panc02 or senPanc02. Representative image (left panel) and quantification (right panel) of *n*=3 independent experiments are shown. **p<0.01; one-way ANOVA test compared to control Panc02 cells.

C. Haematoxylin-eosin (H&E) in skin sections of animals after 7 days of subcutaneous injection of vehicle, control, ICD or senB16F10. Note that the brown pigmentation is due to the melanin. Representative images selected by a histopathologist of *n*=3-5 animals per group are shown. Scale bars for each images are shown (100, 1000, 250, and 250 µm, respectively).

D. Immunohistochemistry of $CD45^+$ cells (purple) in skin sections of animals after 7 days of subcutaneous injection of vehicle, control, ICD or senB16F10. Note that the brown pigmentation is due to the melanin. Representative images selected by a histopathologist of *n*=5 animals per group are shown. Scale bars for each images are shown (100 µm).

E. Immunohistochemistry of $CD3^+$ cells (purple) in skin sections of animals 7 days after subcutaneous injection of vehicle, control, ICD or senB16F10. Note that the brown pigmentation is due to the melamine. Representative images selected by a histopathologist of *n*=5 animals per group are shown. Scale bars for each images are shown (100 µm).

F. In vivo imaging detection of luciferase–expressing B16F10 (B16-luc) in animals subcutaneously injected with vehicle, 10^6 ICD-B16-Luc or $2x10^5$ senB16-Luc (*n*=6-7 per group) at different time points after subcutaneous injection (as indicated). Representative images (left panels) and quantification (right panel) are shown. ***p<0.001, **p<0.01; two-way ANOVA test.

G. Flow cytometry analysis of the DC activation markers CD80, CD86 and MHC-II (I-A/I-B) in $CD11c^+$ BMDCs upon co-culture with RPMI medium either alone or with LPS, B16F10 or senB16F10. Representative histograms and quantification of *n*=3 biological replicates are shown. ***p<0.001, **p<0.01; *p<0.05; one-way ANOVA test.

H. Flow cytometry analysis of the DC activation marker CD80 in $CD11c^+$ BMDCs upon co-culture with RPMI medium either alone or with LPS, B16F10 or senB16F10 using a transwell system. Representative histograms and quantification of *n*=3 biological replicates are shown. ***p<0.001, **p<0.01; *p<0.05; one-way ANOVA test.

I. Flow cytometry analysis of uptake of CFSE (cytosolic dye) or WGA-Alexa647 (membrane dye) by BMDCs from labeled control Panc02, ICD-Pac02 or senPanc02. Quantification after subtraction of autofluorescence from unstained BMDC of *n*=3 biological replicates. ***p< 0.001; **p<0.01 ; *p<0.05, one-way ANOVA test.

J. Flow cytometry analysis of OT-I CD8 T cells activation, as measured by CD69 expression, upon co-culture with RPMI medium either alone or with PMA+I, naïve BMDCs or BMDCs previously co-cultured with B16F10-OVA (B16-OVA) or with senB16F10-OVA (senB16OVA), as indicated. Representative histograms and quantification of *n*=3 biological replicates are shown. ***p<0.001, **p<0.01; *p<0.05; one-way ANOVA test.